








Article

Structural, Mechanical and Electrical Characteristics of Copper Coatings Obtained by Various Electrodeposition Processes

Ivana O. Mladenović ^{1,*}, Marko V. Bošković ¹, Marija M. Vuksanović ², Nebojša D. Nikolić ¹,
Jelena S. Lamovec ³, Dana G. Vasiljević-Radović ¹ and Vesna J. Radojević ⁴

¹ Institute of Chemistry, Technology and Metallurgy, University of Belgrade, Njegoševa 12, 11000 Belgrade, Serbia; boskovic@nanosys.ihtm.bg.ac.rs (M.V.B.); nnikolic@ihtm.bg.ac.rs (N.D.N.); dana@nanosys.ihtm.bg.ac.rs (D.G.V.-R.)

² Institute of Nuclear Sciences, National Institute of the Republic of Serbia, University of Belgrade, Mike Petrovića Alasa 12-14, 11000 Belgrade, Serbia; marija.vuksanovic@vin.bg.ac.rs

³ University of Criminal Investigation and Police Studies, Cara Dušana 196, Zemun, 11000 Belgrade, Serbia; jelena.lamovec@kpu.edu.rs

⁴ Faculty of Technology and Metallurgy, University of Belgrade, Karnegijeva 4, 11000 Belgrade, Serbia; vesnar@tmf.bg.ac.rs

* Correspondence: ivana@nanosys.ihtm.bg.ac.rs; Tel.: +381-11-262-8587

Abstract: Mechanical (hardness and adhesion) and electrical (sheet resistance) characteristics of electrolytically produced copper coatings have been investigated. Morphologies of Cu coatings produced galvanostatically at two current densities from the basic sulfate electrolyte and from an electrolyte containing levelling/brightening additives without and with application of ultrasound for the electrolyte stirring were characterized by SEM and AFM techniques. Mechanical characteristics were examined by Vickers microindentation using the Chen–Gao (C–G) composite hardness model, while electrical characteristics were examined by the four-point probe method. Application of ultrasound achieved benefits on both hardness and adhesion of the Cu coatings, thereby the use of both the larger current density and additive-free electrolyte improved these mechanical characteristics. The hardness of Cu coatings calculated according to the C–G model was in the 1.1844–1.2303 GPa range for fine-grained Cu coatings obtained from the sulfate electrolyte and in the 0.8572–1.1507 GPa range for smooth Cu coatings obtained from the electrolyte with additives. Analysis of the electrical characteristics of Cu coatings after an aging period of 4 years showed differences in the sheet resistance between the top and the bottom sides of the coating, which is attributed to the formation of a thin oxide layer on the coating surface area.

Keywords: copper; electrodeposition; morphology; microstructure; composite hardness; adhesion; critical reduced depth; sheet resistance



Citation: Mladenović, I.O.; Bošković, M.V.; Vuksanović, M.M.; Nikolić, N.D.; Lamovec, J.S.; Vasiljević-Radović, D.G.; Radojević, V.J. Structural, Mechanical and Electrical Characteristics of Copper Coatings Obtained by Various Electrodeposition Processes. *Electronics* **2022**, *11*, 443. <https://doi.org/10.3390/electronics11030443>

Academic Editor: Zhiyuan Zhu

Received: 30 December 2021

Accepted: 29 January 2022

Published: 1 February 2022

Publisher's Note: MDPI stays neutral with regard to jurisdictional claims in published maps and institutional affiliations.



Copyright: © 2022 by the authors. Licensee MDPI, Basel, Switzerland. This article is an open access article distributed under the terms and conditions of the Creative Commons Attribution (CC BY) license (<https://creativecommons.org/licenses/by/4.0/>).

1. Introduction

The integration of new materials and technologies in order to reduce the existing size of electronic devices is a great challenge. It is generally known [1] that with a change in the dimension of a material, there is a drastic change in quality of the material and its specific properties. The copper electroplating, electroforming or electroless techniques are very useful in the semiconductor industry for die stacking and 3D interconnections, chip metallization, damascene interconnection with low resistivity and higher electromigration resistance than Al interconnections, for claddings, barrier and seed layer applications. Electrochemical coatings are used in transistors to form SOI (silicon on isolator) by employing porous silicon to reduce transistor leakage [2].

For all aforementioned applications, a good coating quality at the micro- or nano-levels is required, and electrodeposition processes are very suitable to reach it. Various processes of copper electrodeposition on different bulk materials were developed for

micro electro mechanical systems devices (MEMS), through-hole plating for printed circuit boards (PCBs), as well as for all other conventional functional plating processes on silicon, brass, steel, copper, etc. [3–5]. Copper coatings are the most commonly used material for interconnections within microelectronics. However, limited application of this coating in nanoelectronics is reflected in the high resistance of the material and electromigration [1].

Morphological and mechanical features of electrodeposited copper coatings depend on the type and composition of electrolyte, regime of electrodeposition, intensity of the current density, the presence of specific substances in the electrolyte known as additives for levelling and brightening, electrolyte mixing conditions, etc. [6]. The most commonly used additives in Cu electrodeposition from sulfate electrolytes are: chloride ions, bis(3-sulfopropyl) disulfide (SPS), polyethylene glycol (PEG), 3-mercapto-1-propanesulfonic acid (MPSA), Janus Green B, thiourea, etc. [5,7–11]. It was shown recently [5] that a combination of the additives such as chloride ions, PEG and MPSA added to the basic sulfate electrolyte drastically affected a change of the topography of the copper coatings compared to the coatings obtained from the basic sulfate electrolyte.

It is well known [7,9,12,13] that a quality of electrochemical coatings can be improved by variation of electrolyte mixing conditions, such as application of magnetic and ultrasonic mixing or by barboting. Application of ultrasound (US) in the electrodeposition processes has many benefits: charge-transfer improvement, higher cathode current efficiency, reduction grain size, improvement corrosion and wear resistance, reduction of cathodic polarization, etc. [7,9,12,13].

One of the most important mechanical properties of metal films and coatings is microhardness, which is closely dependent on processing electrodeposition parameters used for their production [14–16]. Assessing the mechanical properties of the coating for electronics is of interest due to the life time of the electronic components. Since an influence of the hardness of the substrate cannot be ignored with the high applied loads, the electrolytically produced copper coatings on the conductive substrates represent a unique composite system from the point of view of consideration of their microhardness. A quality of the coating itself, including size of the grains, preferred orientation, texture, packaging and roughness also affect the assessment of microhardness. A large number of mathematical composite hardness models have been developed so far to determine the “intrinsic” or absolute hardness of film or coating [17–28]. Choosing an adequate mathematical model for calculating the absolute hardness of the coating from the value of composite hardness depends mostly on the type of composite system (“soft film on hard substrate” or “hard film on soft substrate”) [16,29].

Another important mechanical property of interest for the development of microstructure components is the adhesion between layers, i.e., between coating and substrate (cathode). In this paper, the assessment of adhesion between copper coating and substrate was done on the basis of a composite hardness model Chen–Gao and a change in the value of the critical reduced depth (adhesion parameter, b) [23–26,28,30–32]. The basis of the theory of the composite hardness model according to Chen–Gao (C–G) is given in Appendix A.

The knowledge of electrical resistivity is also very important for application of copper coatings in the electronics industry. In the last time, copper replaces aluminum as an interconnecting material due to lower bulk electrical resistivity ($\rho_{Cu} = 1.67 \mu\Omega \text{ cm}$ vs. $\rho_{Al} = 2.65 \mu\Omega \text{ cm}$), higher melting temperature ($T_{Cu} = 1360 \text{ K}$ vs. $T_{Al} = 930 \text{ K}$), better electromigration resistance and higher resistance under stress failures [33]. It is well known that the electrical resistivity of mono-layered thin metallic coatings increases with decreasing coating thickness and it is greater than that of the bulk material [34]. The polycrystalline films are built up of small grains where the electrons can be scattered at the grain boundaries [33,34].

The measured values of sheet resistance of coating (Ω/\square) depend on the coating thickness, surface morphology, type of used substrate, as well as of kind of post-treatment process (annealing) [33–35]. For example, the sheet resistance for the Cu coating produced on Si substrate in the DC mode at a current density of 50 mA cm^{-2} with a thickness of

20 μm was $1.17 \mu\Omega/\square$ before annealing process, and $0.786 \mu\Omega/\square$ after annealing [35]. It was shown [36] that the electrical resistivity of electroless copper films on glass substrate decreases with increasing the film thickness (52.2–982 nm) and the surface roughness or grain size (15.5–28.3 nm). It is also stated that the main factor in increasing the electrical resistivity of nanocrystalline copper films is an increase grain boundaries number.

In this study, mechanical (hardness and adhesion) and electrical (the sheet resistance) properties of Cu coatings obtained under various electrodeposition conditions were analyzed. Cu coatings were electrodeposited by the galvanostatic regime of the electrodeposition (DC mode) from the basic sulfate electrolyte, and from the electrolyte containing levelling/brightening additives, without and with application of ultrasound (US) for the electrolyte stirring at current densities corresponding to both the mixed activation-diffusion and the full diffusion control of electrodeposition. This is done with the aim to establish relationship among morphological, mechanical and electrical characteristics of the obtained coatings.

2. Materials and Methods

2.1. Electrodeposition of Cu Coatings

Copper coatings were produced using constant galvanostatic regime (DC mode) without and with application of ultrasound (US) for mixing of electrolytes at current densities of 33, 67 and 150 mA cm^{-2} . The electrodeposition process was performed from the following electrolytes [5]:

- (a) 240 g/L $\text{CuSO}_4 \cdot 5 \text{H}_2\text{O}$ + 60 g/L H_2SO_4 ; (electrolyte I) and
- (b) 240 g/L $\text{CuSO}_4 \cdot 5 \text{H}_2\text{O}$ + 60 g/L H_2SO_4 + 0.124 g/L NaCl + 1 g/L PEG 6000 (polyethylene-glycol) + 0.0015 g/L MPSA (3-Mercapto-1-propanesulfonic acid); (electrolyte II).

The electrolytes were prepared using double distilled water and reagents of p.a. quality (Sigma-Aldrich, Darmstadt, Germany). The ultrasonic bath (Bransonic 220 Ultrasonic Cleaner, Branson Cleaning Equipment Company, Shelton, CT, USA) frequency at 40 kHz, was performed for mixing of the electrolyte. The cathode was a brass foil (260 1/2 hard, ASTM B36, 250 μm thick, K&S Engineering, Chicago, IL, USA). A copper plate of cylindrical shape was used as anode. The electrochemical cell was made of cylindrical Pyrex glass (150 mL) with a Teflon holder in order to provide a constant position of the Pyrex glass during the application of ultrasound. Electrodeposition was performed at a temperature of $22.0 \pm 0.50 \text{ }^\circ\text{C}$. The thickness of coatings was 20 μm , and was controlled by the mechanical comparator with electronic reader on display (model: Iskra, type: NP37 (Iskra Avtomatica, Ljubljana, Slovenia) with the accuracy of the vertical shift of $\pm 1 \mu\text{m}$ [5]. All conditions applied for a production of uniform Cu coatings are summarized in Table 1.

Table 1. The conditions of electrodeposition applied for a formation of Cu coatings on the brass substrate. The thickness of coatings: $\delta = 20 \mu\text{m}$; DC—the constant galvanostatic regime; US—application of ultrasound for the electrolyte stirring.

The Type of Electrolyte	The Current Density, ($j/\text{mA cm}^{-2}$)	Regime
electrolyte I	33	DC
electrolyte I	33	DC/US
electrolyte I	67	DC
electrolyte I	67	DC/US
electrolyte II	33	DC
electrolyte II	33	DC/US
electrolyte II	67	DC
electrolyte II	67	DC/US
electrolyte II	150	DC/US

Immediately before structural characterization, the samples were chemically etched in a solution: 2 g $\text{K}_2\text{Cr}_2\text{O}_7$ + 8 mL H_2SO_4 + 4 drops HCl + 100 mL deionized water, during 15 s in order to reveal the grain boundaries [37].

2.2. Characterization of Cu Coatings

The copper coatings obtained under various conditions of the electrodeposition were characterized by application of the following techniques:

- (a) The microstructure (morphology) of Cu coatings electrodeposited on the brass substrate was examined using a field emission scanning electron microscope—FESEM, MIRA3 TESCAN XMLI, operated at 20 kV,
- (b) Image analysis of SEM micrographs was undertaken by Image Pro Plus 6.0 software with the aim to determine diagonals of the micro indents used in calculation of hardness values and the grain size distribution.
- (c) The topography of coatings was investigated using an atomic force microscope in the non-contact mode (AFM-Auto Probe CP Research; TM Microscopes-Veeco Instruments, Santa Barbara, CA, USA). The scan area was $(10 \times 10) \mu\text{m}^2$. The image analysis was performed with the WSxM 4.0 software beta 9.3 version [38]. A histogram of topography was generated by the same software.
- (d) The Vickers microhardness tester Leitz Kleinert Prufer DURIMET I (Leitz, Oberkochen, Germany) with applied loads (P) in the (0.049–4.903) N range and a dwell time of 25 s was used for a determination of a hardness of the Cu coatings. For each load, three indentations were made and an average diagonal size was calculated.
- (e) The home-made bending test machine, made in our laboratory, was used for delamination (pull-off) of the copper coating from the brass substrate after a sample aging period of four years. The machine was automated and specially constructed for a purpose of examination of adhesion properties of coatings on flexible foils, using the cyclic bending method. The test parameters were the following: maximal number of cycles ($n_c = 1000$), speed of rotation of step motors ($w = 500 \text{ o min}^{-1}$), the pulling force ($F_c = 21 \text{ N}$), speed of timing belt ($v = 9 \text{ m s}^{-1}$) and dimensions of sample were $(110 \times 10) \text{ mm}^2$ with the coating electrodeposition surface area of $(50 \times 4.0) \text{ mm}^2$.
- (f) The sheet resistance after delamination of the copper coatings from the brass substrates, on bending test machine, was measured by the four-point probe method in the room conditions, with a Gwinstek GPS-3030D DC power supply and Keysight 34461A digital multimeter [9]. The copper coatings strips were placed on a microscope glass; first with placing probes at the coating surface on top side and second by placing probes at the bottom side of the coatings (side of the substrate after delamination), (Figure 1c). The final values of the sheet resistance of Cu coatings are calculated as the average values from three individual measurements on every side of the coating surface area.

The scheme of measurement with the four-probe method is given in Figure 1.

Equation (1) was used to obtain sheet resistance R (in Ω/\square) of the copper coatings on both sides [39,40]:

$$R = \frac{\pi}{\ln 2} \cdot \frac{U}{I} = 4.53 \cdot \frac{U}{I} \quad (1)$$

where I (in mA) is the current which was kept constant at 500 mA and passed through the probe tips, and the voltage U (in μV) measured between the inner probe tips.

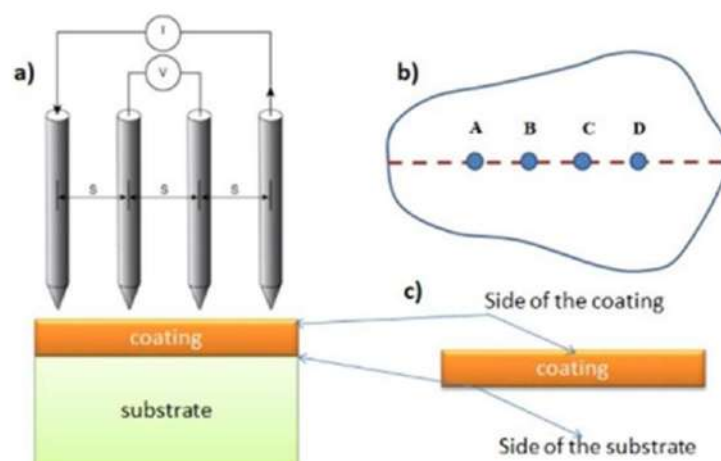


Figure 1. Schematic diagram of four-point probe method: (a) measurement principle, (b) alternative Van der Pauw convention [39] with the four—point probes placed along a symmetry line of samples and (c) measuring points on the coatings surface.

3. Results

3.1. Morphological Analysis of the Copper Coatings Electrodeposited on the Brass Cathode

Figure 2 shows the morphology of 20 μm thick Cu coatings obtained from the basic sulfate electrolyte (electrolyte I) at current densities of 33 and 67 mA cm^{-2} , without (Figure 2a,b,e,f) and with ultrasound assistance (Figure 2c,d,g,h). As seen from this Figure, the fine-grained Cu coatings were obtained at the both current densities. The Cu coatings produced at a current density of 33 mA cm^{-2} without and with ultrasonic mixing of the electrolyte were very similar to each other (Figure 2a–d). On the other hand, application of ultrasound for the electrolyte mixing during electrodeposition at j of 67 mA cm^{-2} led to formation of more compact Cu coating than that obtained without applied ultrasound (Figure 2e–h).

The histograms giving the grain size distribution, generated from SEM micrographs shown in Figure 2 by use of an image processing program, are shown in Figure 3. The histograms shown in Figure 3 reveal the microcrystalline character of these coatings with a content of individual grain sizes in fractions between 1 and 5 μm . At the first sight, it can be noticed that the grain size distributions for the Cu coatings obtained at j of 33 mA cm^{-2} and that obtained at j of 67 mA cm^{-2} in the silent electrolyte were mutually similar with the approximately size of grains in the (2–4) μm range. Consequently, grain size for the microcrystalline Cu coating obtained at j of 67 mA cm^{-2} in the presence of ultrasound was shifted toward lower values, since the increased share of grains size between 1 and 2 μm was noted.

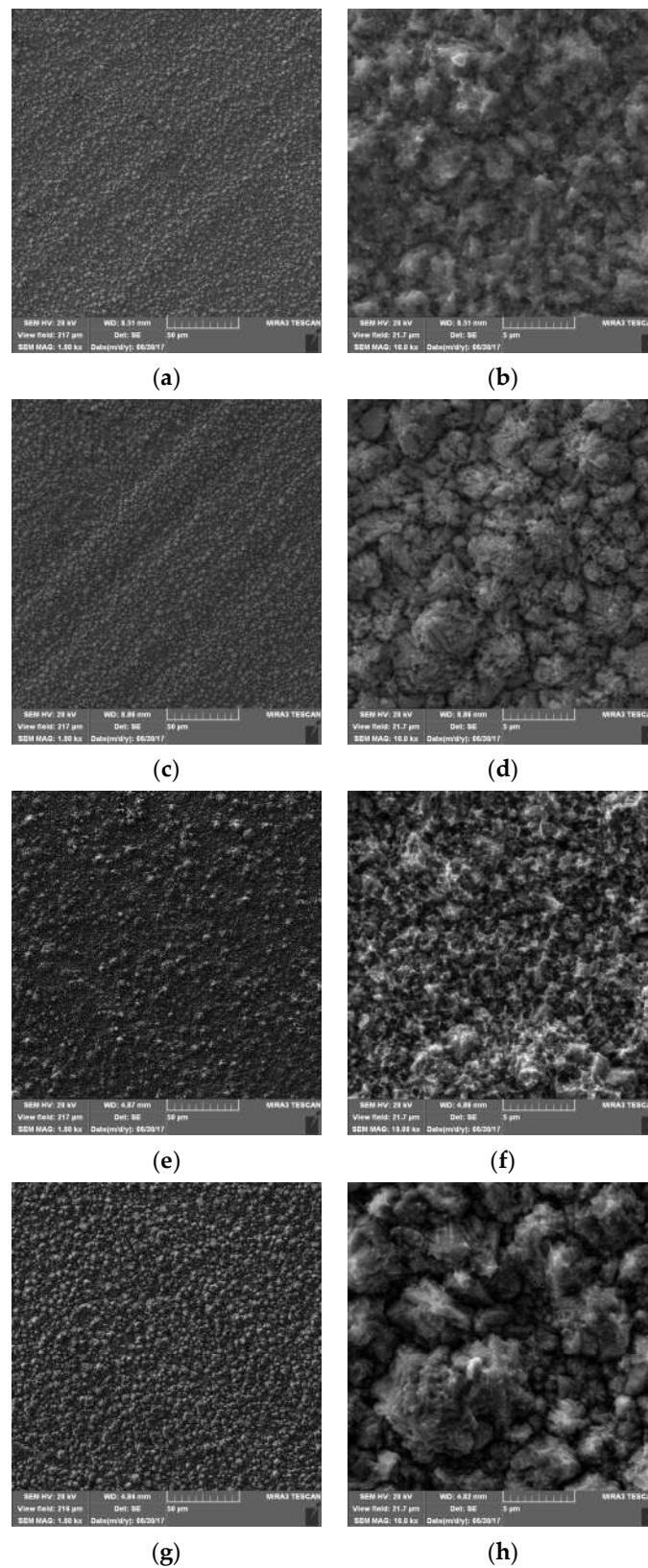


Figure 2. The morphology of 20 μm -thick Cu coatings obtained by electrodeposition from the basic sulfate electrolyte on the brass substrate in the galvanostatic regime (DC) without and with ultrasonic mixing of the electrolyte (US). Magnification: $\times 1000$ (left) and $\times 10,000$ (right): (a,b) DC; $j = 33 \text{ mA cm}^{-2}$, (c,d) DC/US; $j = 33 \text{ mA cm}^{-2}$, (e,f) DC; $j = 67 \text{ mA cm}^{-2}$, and (g,h) DC/US; $j = 67 \text{ mA cm}^{-2}$.

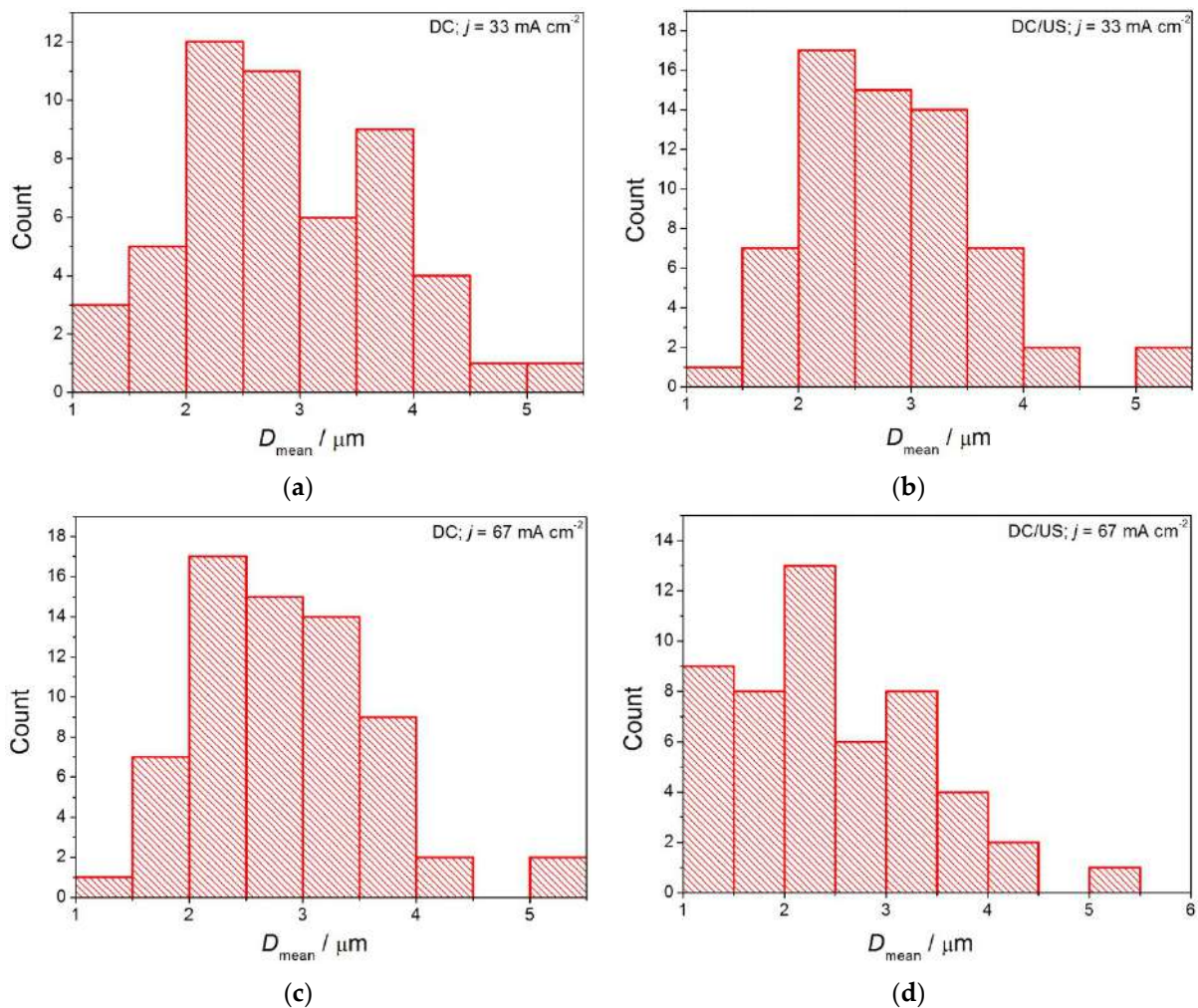
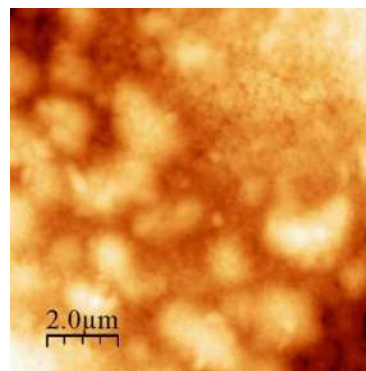


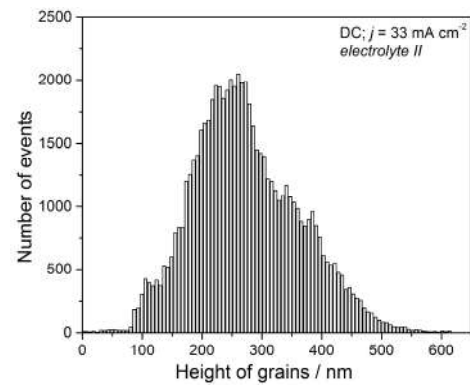
Figure 3. Distribution histogram of the mean diameter of grain size produced copper coatings on the brass substrate in the galvanostatic regime without and with application of ultrasound: (a) DC; $j = 33 \text{ mA cm}^{-2}$, (b) DC/US; $j = 33 \text{ mA cm}^{-2}$, (c) DC; $j = 67 \text{ mA cm}^{-2}$ and (d) DC/US; $j = 67 \text{ mA cm}^{-2}$.

When it comes to morphological analysis of the Cu coatings produced from the electrolyte with an addition of levelling/brightening additives (electrolyte II), the SEM technique in a combination with the image processing program was not reliable. The addition of the additives affects a reduction of the grain size in the coatings up to the order of a few hundred nanometers and the grain boundary in them is not clearly visible [5]. Unlike the microcrystalline coatings obtained from the basic sulfate electrolyte, the Cu coatings obtained from the electrolyte containing levelling/brightening additives represent the typical nanocrystalline coatings [5]. These coatings are smooth, with mirror bright appearance and, as already stated, without a clear boundary among grains. For that reason, topography and the estimation of grain size distribution (histogram of the topography) of these coatings was undertaken by the application of the AFM technique.

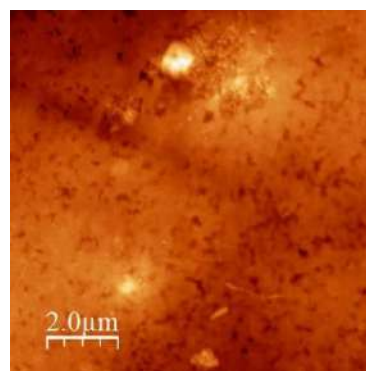
The AFM surface areas and histograms of the topography of mirror bright Cu coatings produced from the electrolyte with additives (electrolyte II) without and with applied ultrasound at current densities of 33 and 67 mA cm^{-2} are shown in Figure 4a–h.



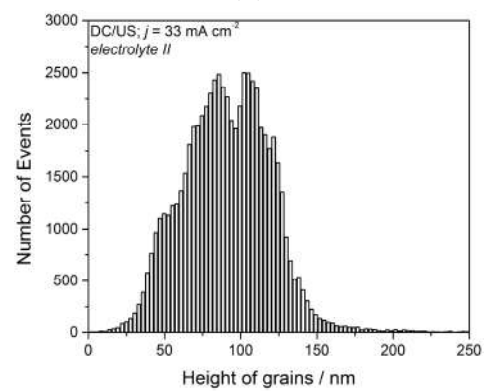
(a)



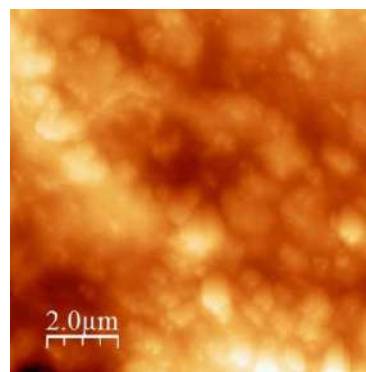
(b)



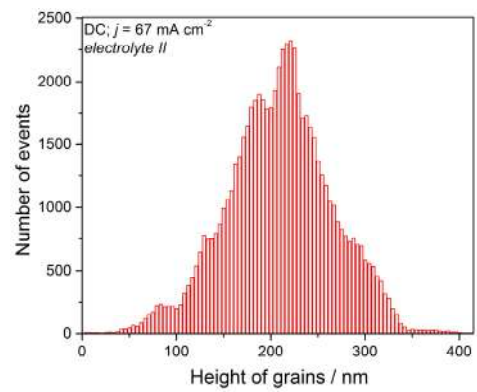
(c)



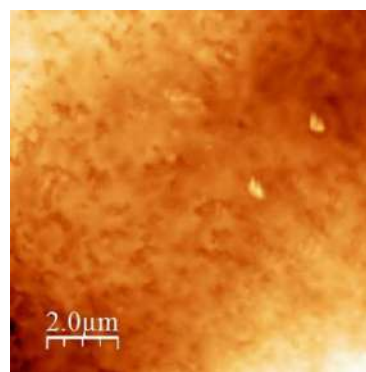
(d)



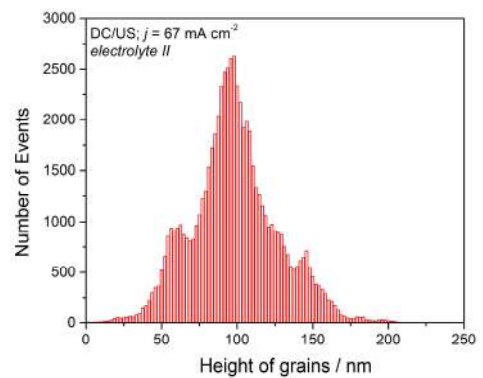
(e)



(f)



(g)



(h)

Figure 4. Cont.

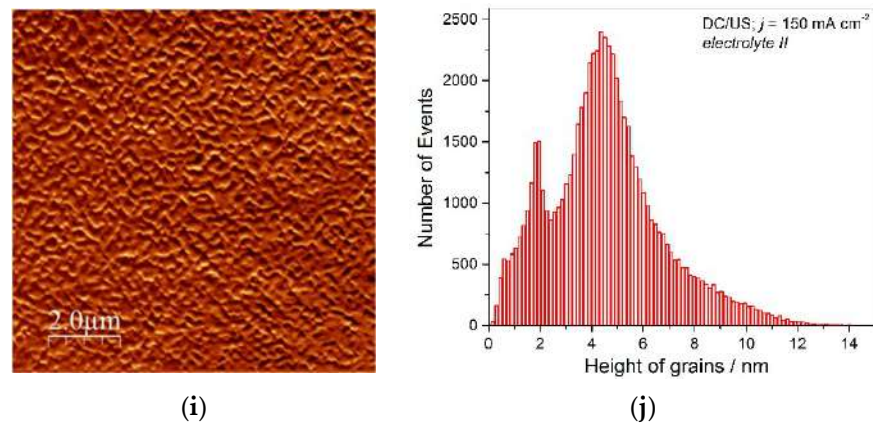


Figure 4. The surface topography and histogram of topography of 20 μm thick Cu coatings obtained by the DC mode from electrolyte II without and with application of ultrasound (US) for mixing of the electrolyte at current densities of: (a,b) DC; $j = 33 \text{ mA cm}^{-2}$, (c,d) DC/US; $j = 33 \text{ mA cm}^{-2}$, (e,f) DC; $j = 67 \text{ mA cm}^{-2}$, and (g,h) DC/US; $j = 67 \text{ mA cm}^{-2}$, (i,j) DC/US; $j = 150 \text{ mA cm}^{-2}$. Scan size: $(10 \times 10) \mu\text{m}^2$.

The Cu coatings obtained from electrolyte II with applied ultrasonic mixing of the electrolyte (Figure 4c,g) were of a more uniform topography than those obtained without an application of ultrasound (Figure 4a,e). For this electrolyte type, more uniform surface topography with applied ultrasound is obtained at the both current densities, that was also confirmed by histogram analysis. The height of grains for the Cu coatings obtained with ultrasonic electrolyte mixing was about 100 nm (Figure 4d,h), while for those obtained without it was larger than 200 nm (Figure 4b,f).

The AFM surface area and histogram of the topography of the Cu coating produced at a current density of 150 mA cm^{-2} from electrolyte II in the presence of ultrasound are shown in Figures 2i and 2j, respectively. At first sight, the topography of this coating was to a certain extent different than those obtained at the lower current densities. The height of grains in this coating was about twenty times smaller than that obtained at j of 67 mA cm^{-2} , and about 40 times smaller than that obtained at j of 33 mA cm^{-2} .

3.2. Analysis of Mechanical Properties of the Copper Coatings Electrodeposited on the Brass Cathode

The dependencies of the composite hardness (H_c) calculated according to Equation (A5) from Appendix A on the relative indentation depth (RID) for Cu coatings obtained from electrolyte I are shown in Figure 5a, while for those obtained from electrolyte II are shown in Figure 5b. The RID is defined as a ratio between an indentation depth, h and a coating thickness, δ ($\text{RID} = h/\delta$). The shapes of the H_c -RID dependencies obtained for the electrolyte I and II are different. For the electrolyte I, H_c increases with the increasing RID value up to certain critical value corresponding to the RID value of about 0.14, and then, it decreases reaching approximately the value of hardness of the brass substrate (H_s) of 1.41 GPa [5] (Figure 5a). For the electrolyte II, there is continuous growth in the H_c on the RID in the whole RID range, and it is important to note that the value of the hardness of the brass substrate was not reached for all Cu coatings (Figure 5b).

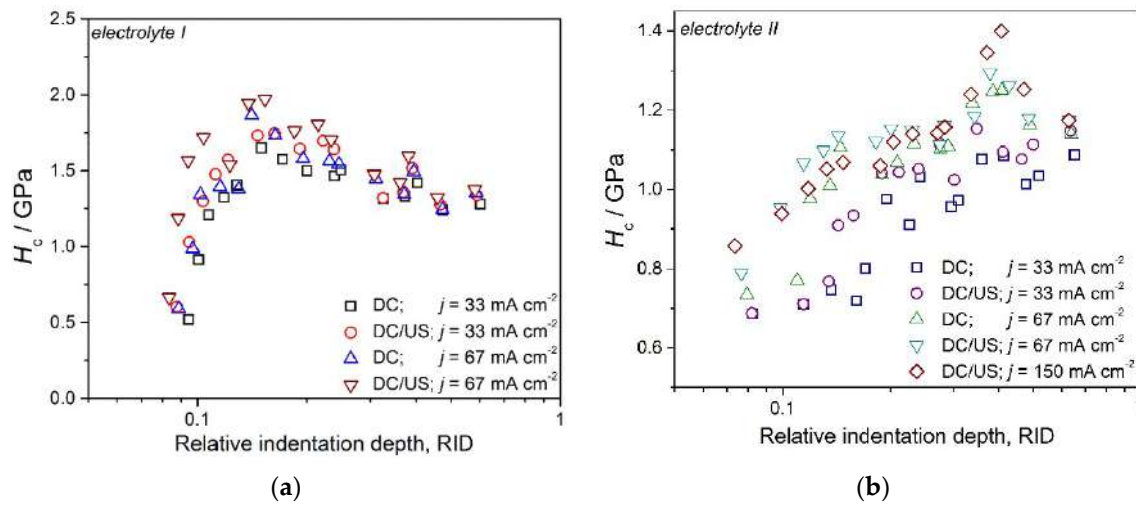


Figure 5. The variation of the composite hardness values with relative indentation depth for 20 μm thick copper coatings electrodeposited on the brass substrate in DC or DC/US regime with applied current densities of 33, 67 and 150 mA cm^{-2} from: (a) electrolyte I and (b) electrolyte II.

We can see from Figure 5 that the composite hardness values obtained for the copper coatings in the DC/US regime were larger than those obtained in the DC regime at both applied current densities (33 and 67 mA cm^{-2}). Comparing the dependencies shown in Figure 5a,b, it is clear that the H_c values for the copper coatings produced from the electrolyte II are lower than those obtained for the Cu coatings produced from the electrolyte I. The values of an absolute hardness for each produced copper coating were calculated applying the Chen–Gao (C–G) composite hardness model, and the obtained values are summarized in Table 2. Fitting of experimental microhardness data according to the C–G model as the dependencies of the composite hardness on depth of the indentation are shown in Figure 6. Figure 6a shows the fitting curves for the Cu coatings produced from electrolyte I, while Figure 6b shows the same dependencies obtained for electrolyte II. This fitting was done in MATLAB program using the cftool command according to Equation (A3) and then an absolute hardness of the coatings was estimated according to the Equation (A4) given in Appendix A.

Table 2. The results of calculated absolute hardness of the Cu coatings, H_{coat} (in GPa), produced on the brass substrate, together with both fitting parameters (A , B , C) and root mean square error (RMSE) values.

$j/\text{mA cm}^{-2}$	Regime	Electrolyte	A	B	C	RMSE	$H_{\text{coat}}/\text{GPa}$
33	DC	I	1.249	−7.608	59.06	0.05891	1.1844
33	DC/US	I	1.216	−10.23	324.2	0.05912	1.1864
67	DC	I	1.223	−1.242	−245.5	0.04471	1.2123
67	DC/US	I	1.267	−4.835	−103.5	0.06704	1.2303
33	DC	II	0.872	27.83	−3236	0.08048	0.8572
33	DC/US	II	0.877	30.04	−3007	0.07452	0.8721
67	DC	II	0.902	32.04	−2718	0.8851	0.8851
67	DC/US	II	0.927	27.40	−2871	0.9119	0.9119
150	DC/US	II	1.176	−5.437	228.1	0.05069	1.1507

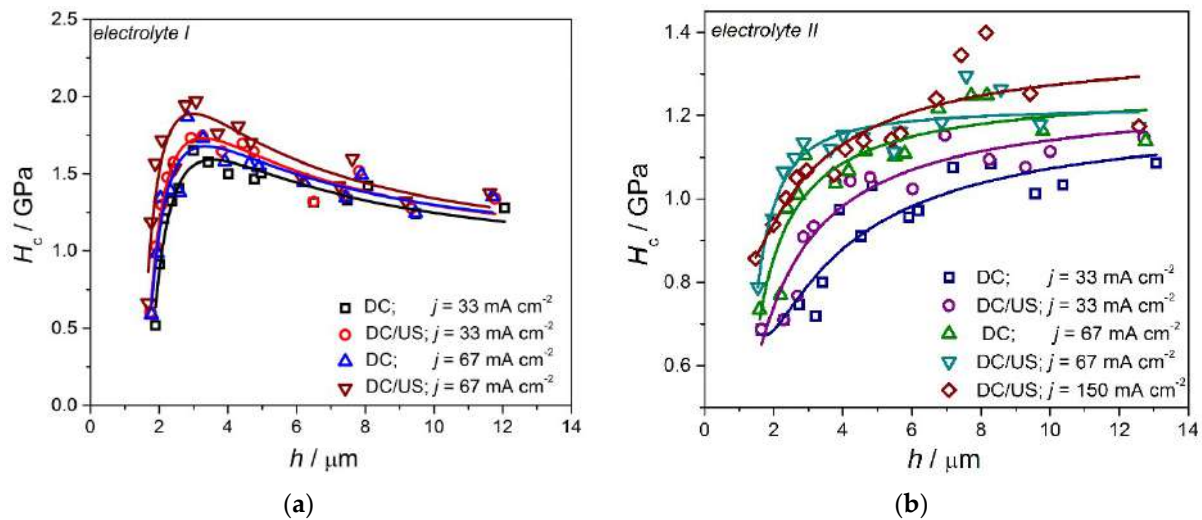


Figure 6. The dependencies of the composite hardness for 20 μm thick copper coatings electrodeposited on the brass substrate, H_c on indentation depth, h calculated according to Chen–Gao model: (a) electrolyte I and (b) electrolyte II.

The values of coating hardness obtained at a current density of 33 mA cm^{-2} from additive-free electrolyte (electrolyte I) without and with application of ultrasound were very similar to each other, that was in line with morphology of the coatings obtained at this current density (Figure 2a–d). As already mentioned, ultrasound had not any significant effect at this current density, causing similar morphologies of Cu coatings. The hardness of coatings obtained at j of 67 mA cm^{-2} was larger than those obtained at j of 33 mA cm^{-2} . The larger value of the coating hardness obtained at j of 67 mA cm^{-2} with applied ultrasound relative to that obtained in the silent electrolyte is due to useful effect of ultrasound waves on electrodeposition process manifested by formation of more refined structure with the smaller grain size in the presence of ultrasound (Figure 3c,d). At both current densities, the hardness of the coatings obtained from the electrolyte containing additives (electrolyte II) was smaller than those obtained from additive-free electrolyte (electrolyte I), that can be ascribed to phenomena on the grain boundary [5].

Taking in consideration correlation between a diagonal size, d , and indentation depth, h , as $d = 7h$ for a Vickers hardness tester [41] and $\Delta H = H_s - H_c$, the Equation (A2) in Appendix A, becomes:

$$\Delta H = \left[\frac{7 \cdot (n + 1) \cdot (H_s - H_{\text{coat}})}{n \cdot b} \right] \cdot \frac{\delta}{d} \quad (2)$$

Equation (2) was used to calculate the critical reduced depth, b , parameter representing an estimation of adhesion of any coating with substrate [23–26,30–32]. The value of the parameter n in Equation (2) is either 1.2 or 1.8, and for “soft coatings on hard substrate” like the Cu coatings on the brass substrate analyzed here, the value n of 1.8 was taken [26,30]. In this calculation, the value of hardness of the brass substrate (H_s) of 1.41 GPa [5] was taken, while the values of the absolute hardness calculated according to C–G model (Table 2) were taken for a determination of ΔH in the Equation (2). The dependencies of ΔH on δ/d for the Cu coatings obtained from the electrolyte II are given in Figure 7. The adhesion parameter, b was calculated from slope of the linear dependencies shown in this Figure, and the calculated values are given in the Table 3. The larger value of the adhesion parameter b means the better adhesion of the coating with substrate [23–26,30–32].

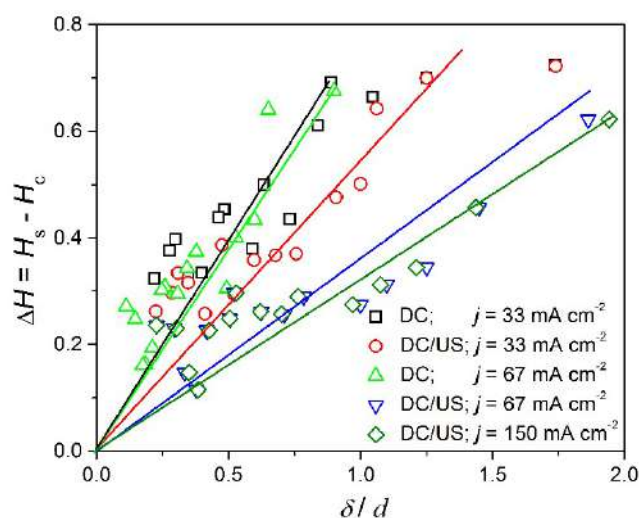


Figure 7. The hardness difference versus ratio between the coating thickness and the diagonal size for the copper coatings electrodeposited on the brass substrate from electrolyte II at two different current densities without and with the application of ultrasound.

Table 3. The results of calculated critical reduced depth, b , according to the Chen–Gao composite hardness model.

$j/\text{mA cm}^{-2}$	Regime	Electrolyte	Slope, k	Parameter, b
33	DC	II	0.79	7.64
33	DC/US	II	0.54	10.8
67	DC	II	0.76	8.64
67	DC/US	II	0.36	15.0
150	DC/US	II	0.37	7.63

From Table 3, it can be seen that the Cu coatings obtained at 33 and 67 mA cm^{-2} with ultrasound stirring of the electrolyte showed better adhesion than those obtained without the electrolyte stirring. This was in agreement with already published results [42], where the improvement of coating adhesion with an application of ultrasound was observed by the scribe-grid test. Simultaneously, the weakest adhesion with the cathode surface showed the Cu coating produced at a current density of 150 mA cm^{-2} from electrolyte II with ultrasonic stirring of the electrolyte.

3.3. The Sheet Resistance Analysis of the Copper Coatings Electrodeposited on the Brass Cathode

In order to examine an influence of natural oxidation of electrodeposited copper coatings on their electrical properties, the sheet resistance, R in (Ω/\square), of the obtained coatings was measured by the four-point probe method after an aging period of 4 years. Measurements by the four-point probe method [43] were performed as shown in Figure 1, on the surface area of the coating (top side) and on the surface area of the coating on the substrate side after delamination (bottom side). Equation (1) was used for a calculation of the sheet resistance on both sides of the copper coatings. The values of sheet resistance of Cu coatings obtained on top side (R_{top}) and bottom side (R_{bot}) are given in Table 4. For the Cu coatings obtained at j of 33 and 67 mA cm^{-2} , the obtained values were in the line with those found in the literature [33–36]. The values obtained at j of 150 mA cm^{-2} were considerably lower than those obtained at j of 33 and 67 mA cm^{-2} , that will be commented on in the Discussion section. Also, it is very clear that the sheet resistance on the top side of the copper coating has higher value than that on the bottom side for all samples. This behavior is expected because the bottom side of the coating was protected from a possible oxidation in the air by the substrate. One of the ways of decreasing the sheet resistance on the top side of the copper coating is a protection of this coating side by immersion in

solution of an active substance which inhibits the corrosion of copper surface area [44]. The typical active substances used for protection or stabilization of the copper surface area are: benzoic acid, benzotriazole, sodium soap and K–Na tartarate. Certainly, this will be examined in detail in a further investigation.

Table 4. The values of the sheet resistance for delaminated copper coatings after aging period of four years measured on top coating side, R_{top} , and on bottom side, R_{bot} , U_{top} , U_{bot} —the voltage in μV measured between the inner probe tips on top or bottom side of the coating.

J (mA cm^{-2})	Regime	Electrolyte	U_{top} (μV)	U_{bot} (μV)	R_{top} ($\text{m}\Omega/\square$)	R_{bot} ($\text{m}\Omega/\square$)
33	DC	I	258	250	2.34	2.27
33	DC/US	I	264	255	2.39	2.31
33	DC	II	250	248	2.26	2.25
33	DC/US	II	269	255	2.44	2.31
67	DC	I	255	250	2.31	2.27
67	DC/US	I	260	255	2.36	2.31
67	DC	II	243	240	2.20	2.17
67	DC/US	II	250	245	2.27	2.22
150	DC/US	II	108	102	0.98	0.92

4. Discussion

Independent of use of ultrasound for the electrolyte mixing, the two types of Cu coatings were formed: the fine-grained microcrystalline (mc) coatings were obtained from the basic sulfate electrolyte (electrolyte I), and the smooth nanocrystalline (nc) coatings were obtained from the electrolyte with addition of levelling and brightening additives (electrolyte II).

Formation of surface morphologies from the basic sulfate electrolyte (Figure 2) can be explained in the following way: for this Cu electrolyte, both current densities belong to the mixed activation-diffusion control [45,46], whereby a contribution of the activation control in the mixed activation-diffusion control decreases with increasing the current density. Application of ultrasound causes a formation of cavitation bubbles, which collapse on the cathode and promote electrolyte mixing in the near-electrode layer [42]. This process is accompanied by the decrease of the thickness of the diffusion layer, and it is a primary characteristic of the diffusion controlled electrodeposition process [6]. At a current density of 33 mA cm^{-2} , a contribution of the activation control is dominant, and for that reason, application of ultrasound had not any effect on morphology of the Cu coatings. Opposite to this current density, a contribution of diffusion to the mixed control of the electrodeposition process is significant at a current density of 67 mA cm^{-2} , leading to useful effect of ultrasound waves on morphology of the coating. As result of this process, more compact and more uniform Cu coating with the smaller grain size in the (1–3) μm range is formed at a current density of 67 mA cm^{-2} with the application of ultrasound than that formed without it, when the grain size was in the (2–4) μm range. The good levelling effect of the additives on the Cu electrodeposition process from the electrolyte containing additives was enhanced by application of ultrasound. The decrease of height of grains for approximately double was observed by application of the ultrasound at the both current densities.

Unlike current densities of 33 and 67 mA cm^{-2} belonging to the mixed activation-diffusion control, a current density of 150 mA cm^{-2} belongs to the full diffusion control of the electrodeposition [45]. In non-stirred electrolytes, the powdered deposits form in this type of the electrodeposition control from all types of electrolyte [6]. The compact, but very rough deposit, was formed from the basic sulfate electrolyte with imposed ultrasonic mixing of the electrolyte. For these reasons, analysis of mechanical and electrical properties of these deposits was not possible.

Analysis of the histograms obtained for the Cu coatings from the electrolyte containing additives (electrolyte II) with the applied ultrasound at current densities of 33, 67 and 150 mA cm^{-2} (Figure 4d,h,j) showed that height, and hence, size of grains decreased with increasing the current density of the electrodeposition. This decrease in grain size can be

explained by the basic nucleation law [6], predicting an increase of nucleation rate with increasing current density (or potential) of the electrodeposition. It means that a larger number nucleus is formed in the initial stage of electrodeposition at j of 150 mA cm^{-2} than at j of 33 and 67 mA cm^{-2} leading to a formation of nanocrystalline coating with a larger number of smaller Cu grains.

Similar to the morphology of the Cu coatings, the largest effect on crystal structure (i.e., on the preferred orientation of coating) has the type of electrolyte [5,47]. In both the constant (potentiostatic and galvanostatic) regimes of electrodeposition, the Cu coatings obtained from the basic sulfate electrolyte possessed the (220) preferred orientation, and this preferred orientation did not depend on applied current density or potential, type of cathode used, and concentrations of both Cu(II) ions and sulfuric acid as constituents of the sulfate electrolyte [4,5,48,49]. On the other hand, the mirror bright Cu coatings obtained here used levelling and brightening additives exhibited the strong (200) preferred orientation [5,47]. This preferred orientation was caused by the synergetic effect of the additives on the Cu electrodeposition process (model “local perforation”) [50,51].

Various morphologies of the Cu coatings obtained under various electrodeposition conditions strongly affected their mechanical characteristics. With a hardness of brass substrate of 1.41 GPa, the Cu coatings on it are classified into the group of “soft film on hard substrate” composite system type [5,16,45,46]. The values of coating hardness calculated by the C–G model were in the 1.1844–1.2303 GPa range for the Cu coatings obtained from electrolyte I and in the 0.8572–1.1507 GPa range for those obtained from the electrolyte II. The calculated values were in an excellent agreement with those obtained for the Cu coatings produced on the same substrate by the pulsating current (PC) regime [46]. The larger values of the composite hardness produced for the coatings obtained from the additive-free electrolyte than those obtained for the coatings produced from the electrolyte with additives can be explained by phenomena on the grain boundary, as already considered for the Cu coatings electrodeposited on the brass and Si(111) substrates from the same electrolytes with magnetically stirred electrolytes [5]. The maximum on the curves of the dependencies of H_c on RID (Figure 5a) and H_c on h (Figure 6a) corresponds to the RID value of 0.14 or h of approximately $2.8 \mu\text{m}$. By application of the Chicot–Lesage composite hardness model [5,52], the RID value of 0.14 is established as the critical value separating the area in which the composite hardness is equal to the coating hardness rather than the area in which both substrate and coating contribute to the composite hardness.

Aside from the type of electrolyte and the current density applied as considered here, the largest effect on mechanical properties (i.e., hardness) of electrolytically produced Cu coatings had the type of used cathode and the coating thickness. Considering the Cu coatings electrodeposited on hard Si(111) and brass cathodes under the same electrodeposition conditions, it was found [5] that the coating hardness produced on very hard Si(111) substrates was larger than that obtained on the softer brass substrate. This can be explained by the impossibility of complete elimination of contribution of substrate hardness to measured composite hardness by application of the composite hardness models. Simultaneously, the coating hardness decreased with the increasing coating thickness, which can be attributed to the decrease of the contribution of the hard substrate to the measured composite hardness with increasing coating thickness [5,45,46,53]. The same trend of an influence of thickness of the coatings on the coating hardness was also observed for the Cu coatings obtained by the pulsating current (PC) regime [46,53].

The C–G model is also successfully implemented in a quantitative estimation of adhesion of the Cu coatings with the brass substrate (Figure 7). The improvement of adhesion of the coatings obtained under ultrasonic electrolyte stirring relative to those obtained in the silent electrolyte is also observed by the scribe-grid test [42]. The weakest adhesion observed for the Cu coating obtained at 150 mA cm^{-2} is in accordance with the basic postulates of electrocrystallization [6]. Namely, deposits obtained under diffusion-controlled electrodeposition always have weaker adhesion with an electrode surface than those obtained in the mixed activation-diffusion control.

As already shown, the composite hardness of the coatings depends on the applied load (Figures 5 and 6). The load-dependence of composite hardness is called the indentation size effect (ISE) [54–59]. This effect can be modeled in two ways: empirically (according to Meyer’s power law relationship [16,20,57–59]) or according to the *PSR* model [54], i.e., as a linear function between the hardness and the reciprocal value of indentation diagonal. The indentation size effect is clearly visible from the SEM micrographs shown in Figure 8, showing the Vickers’s indents. The formation of a pile-up [27,56–59] at the edge of the indent is clearly visible from Figure 8b for the softer copper coating produced from electrolyte II. The pile-up effect is not visible around the indent for the Cu coating produced from electrolyte I (Figure 8a), where the dominant effect is plastic deformation of the coating under the indenter. This confirms that the Cu coating produced from electrolyte I is harder than the Cu coating produced from electrolyte II.

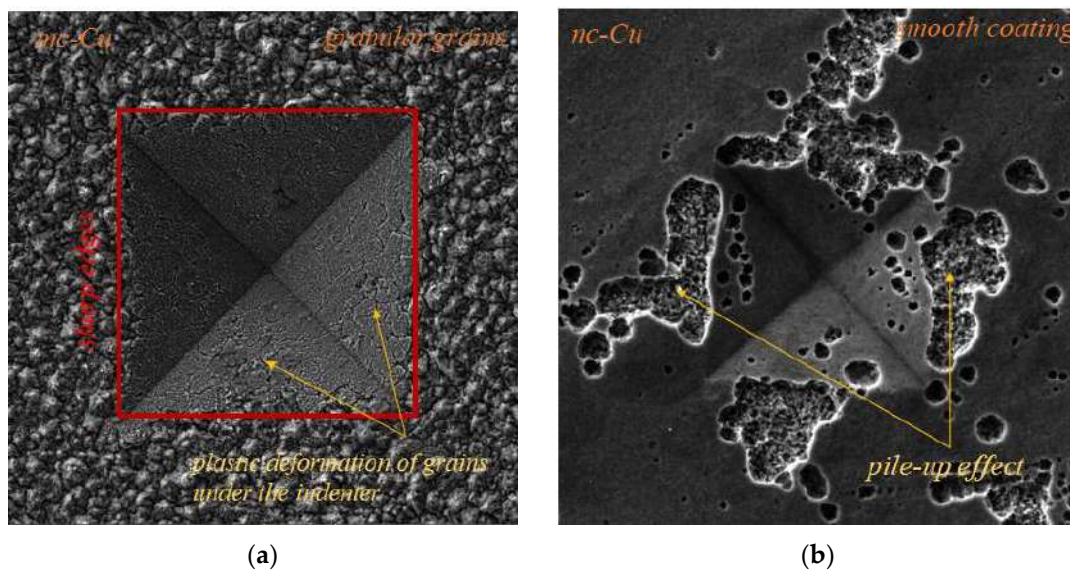


Figure 8. A comparison of deformation of the coatings around an indentation position as a function of the applied load: (a) the Cu coating from electrolyte I (DC, $j = 33 \text{ mA cm}^{-2}$), $P = 4.903 \text{ N}$, $d = 84.4 \text{ }\mu\text{m}$ and (b) the Cu coating from electrolyte II (DC/US, $j = 67 \text{ mA cm}^{-2}$), $P = 0.981 \text{ N}$, $d = 39.6 \text{ }\mu\text{m}$.

When the radius of plastic zone exceeds the coating thickness, both coating and substrate contribute to the measured composite hardness. In the case of the softer Cu coatings produced from electrolyte II, the radius of the plastic zone is larger than the radius of the plastic zone in the coatings produced from electrolyte I and, then, the indentation depth is higher (see Figure 6a,b). The plastic deformation of fine-grained coatings occurs throughout the grain with the slip of dislocations mostly in the grain interior (intragranular slip) [60]. For Cu coatings whose grain size is in the order of nanometers, this mechanism is not possible.

Zhang et al. report that the effects of grain boundaries are significant in raising the electrical resistivity of films or coatings [61]. The Cu coatings obtained from electrolyte I contain a large dislocation density and more grain boundaries compared to bulk copper that rise their electrical resistivity [1]. In the case of lost grain boundaries (the Cu coating produced from electrolyte II) the sheet resistance values are lower than those obtained for Cu coatings from electrolyte I under the same electrodeposition conditions (see Table 4). On the other hand, the use of additives can cause a high level of impurity incorporation into the Cu coating inhibiting self-annealing and reducing the sheet resistance (Zener pinning effect) of the coating [62].

The considerably lower values of the sheet resistance obtained for the Cu coating produced at j of 150 mA cm^{-2} from electrolyte II with an imposed ultrasound can be explained as follows: as already mentioned, a current density of 150 mA cm^{-2} belongs to the diffusion-controlled electrodeposition, probably making the interior of the coating

porous. On the other hand, very compact coatings are formed at j of 33 and 67 mA cm⁻² belonging to the mixed activation-diffusion control of the electrodeposition, causing the higher, and same order of magnitude, values of sheet resistance.

In this study, a detailed analysis of the self-annealing process of electrolytically produced Cu coatings has not been performed, because our main aim was to compare the sheet resistance of the delaminated Cu coatings after a long period of time (in this case, it was a period of 4 years). However, at the first sight it can be mentioned that the observed trend in a change of the sheet resistance was consistent with that found in the literature. The largest resistivity drop by self-annealing process was observed at the low current density, and it decreased with the increasing current density of electrodeposition [63]. For example, the largest drop of resistivity in the Cu coatings from 7.70 to 2.86 $\mu\Omega$ cm is observed when the current density was increased from 1 to 3.33 mA cm⁻². In our case, the larger difference in the sheet resistance between top and bottom sides of the Cu coatings is observed for the Cu coatings produced at 33 mA cm⁻² rather than at 67 mA cm⁻².

Nonetheless, there is a strong dependency of the mechanical and electrical properties on morphological and structural characteristics. Among other things, special attention in future investigations will be devoted to the self-annealing process, and the establishment of its dependency on the morphology and structure of deposits.

5. Conclusions

The influence of parameters of electrodeposition, such as the current density, composition of the electrolyte and the electrolyte mixing (ultrasound) on morphological, mechanical (hardness and adhesion) and electrical (the sheet resistance) characteristics of the Cu coatings has been examined. Scanning electron microscopy (SEM) and the atomic force microscopy (AFM) techniques with accompanying software for imaging analysis were used for morphological characterization of the Cu coatings. Vickers micro indentation was used for mechanical characterization and the four-point probe method was used for characterization of electrical properties of the Cu coatings. On the basis of the obtained results, it was concluded that:

- The fine-grained microcrystalline coatings are obtained from the basic sulfate electrolyte, and the smooth mirror bright nanocrystalline coatings were obtained from the electrolyte containing additives. The use of ultrasound led to a reduction in grain size, especially during electrodeposition from the electrolyte containing additives. For the additive-free electrolyte, reduction in grain size was only observed at a current density of 67 mA cm⁻².
- Application of ultrasound led to an increase in the coating hardness and an improvement of adhesion of coatings with the cathode. The benefits of the application of ultrasound were larger at j of 67 mA cm⁻² than at 33 mA cm⁻². The weakest adhesion with the cathode obtained for the coating produced at 150 mA cm⁻² is explained by the formation of this coating in conditions of the full diffusion control of the electrodeposition.
- Although the values of the sheet resistance obtained at current densities of 33 and 67 mA cm⁻² were in line with those found in the literature, a difference in values on the top and the bottom of the coatings indicated the necessity of additional protection of the coatings from possible oxidation in the air. The lower values of the sheet resistance obtained for the Cu coating produced at j of 150 mA cm⁻² can be attributed to the fact that this current density belongs to the diffusion control of the electrodeposition favoring a formation of smaller compact coatings than those formed in the mixed activation-diffusion control (j of 33 and 67 mA cm⁻²).

Author Contributions: Conceptualization, N.D.N. and I.O.M.; methodology, I.O.M., J.S.L., D.G.V.-R. and M.V.B.; software, M.M.V., D.G.V.-R. and I.O.M.; validation, N.D.N., V.J.R. and J.S.L.; performed experiments and contributed to the analysis of microhardness, I.O.M. and J.S.L.; contributed to the analysis of sheet resistance, M.V.B. and I.O.M.; conceived and wrote the paper, N.D.N. and

I.O.M.; writing—review and editing, N.D.N., V.J.R., J.S.L., M.M.V. and D.G.V.-R.; validation N.D.N., V.J.R., J.S.L. and D.G.V.-R.; visualization, I.O.M., M.M.V. and N.D.N.; supervision, N.D.N., V.J.R. and D.G.V.-R. All authors have read and agreed to the published version of the manuscript.

Funding: This work was financially supported by the Ministry of Education, Science and Technological Development of the Republic of Serbia (Grants No. 451-03-9/2021-14/200026; 451-03-9/2021-14/200135 and 451-03-9/2021-14/200017).

Institutional Review Board Statement: Not applicable.

Informed Consent Statement: Not applicable.

Data Availability Statement: The data presented in this study are available on request from the corresponding author or co-authors. The data are not publicly available.

Acknowledgments: This work was funded by Ministry of Education, Science and Technological Development of Republic of Serbia.

Conflicts of Interest: The authors declare no conflict of interest.

Appendix A

The basis of the Chen–Gao (C–G) composite hardness model.

In the physical sense, the critical reduced depth represents the ratio of the plastic zone radius (r) and indentation depth (h) and is determined by the ratio of elastic Young's modulus (E) to hardness of materials (H), as expressed by Equation (A1):

$$b = \frac{r}{h} \alpha \left(\frac{E}{H} \right)^m \quad (\text{A1})$$

where m is parameter between 0.33 and 0.5 [28]. In all these investigations, a Vickers indentation test was adopted to evaluate the adhesion strength of the copper coatings using a composite hardness model according to the Chen–Gao model [23–25]. Based on this model, composite hardness H_c of the coating–substrate system is expressed by Equation (A2):

$$H_c = H_s + \left[\frac{(n+1) \cdot \delta}{n \cdot b \cdot h} \right] \cdot (H_{\text{coat}} - H_s) \quad (\text{A2})$$

where H_s and H_{coat} are the hardness of the substrate and the coating, respectively, δ is the coating thickness, d is the indentation diagonal, b is the critical reduced depth and m is the power index. The value of n is found to be 1.8 for $H_{\text{coat}} < H_s$ ($n \rightarrow 2$; volume law of mixtures applies) or 1.2 ($n \rightarrow 1$; area law of mixtures applies) for $H_{\text{coat}} > H_s$ [24]. The value of the adhesion parameter b is determined from the slope of the linear fit of the line $\Delta H = f(\delta/d)$. The specified model was also used to evaluate the absolute hardness of the coating (H_{coat}) by fitting experimental composite data with the depth of the indentation (h), based on Equation (A3) [24]:

$$H_c = A + B \cdot \frac{1}{h} + C \cdot \frac{1}{h^{n+1}} \quad (\text{A3})$$

where A , B and C are fitting parameters, calculated from curve fitting. Indentation depth can be calculated as 1/7 of diagonal size ($h = d/7$) as theoretical value according to the geometry of the indenter. Then, coating hardness can be expressed according to Equation (A4) [24]:

$$H_{\text{coat}} = A \pm \sqrt{\frac{[n \cdot |B| / (n+1)]^{n+1}}{n \cdot |C|}} \quad (\text{A4})$$

To apply the specified model, it is not necessary to know the absolute hardness of the substrate; but to evaluate the parameters of adhesion, knowledge of the value of H_s is required. The average values of the indent diagonal, d (in m), were calculated from several independent measurements on every specimen for different applied loads P (in N). The

absolute substrate hardness and composite hardness values, H_c (in Pa) were calculated using Equation (A5) [41]:

$$H_c = \frac{1.8544 \cdot P}{d^2} \quad (\text{A5})$$

where 1.8544 is a constant, geometrical factor for the Vickers indenter. The substrate hardness (H_s) was obtained by measuring Vickers hardness with load variation and applying the PSR (proportional specimen resistance) model [57], before depositing the coatings.

References

1. Read, D.; Volinsky, A. Thin Films for Microelectronics and Photonics: Physics, Mechanics, Characterization, and Reliability. In *Micro- and Opto-Electronic Materials and Structures: Physics, Mechanics, Design, Reliability, Packaging*, 1st ed.; Suhir, E., Lee, Y.C., Wong, C.P., Eds.; Springer Kluwer: Riverwoods, IL, USA, 2007; Volume 4, pp. 135–180. [CrossRef]
2. Dubin, V.M. Electrochemical aspects of new materials and technologies in microelectronics. *Microelectron. Eng.* **2003**, *70*, 461–469. [CrossRef]
3. Cortés, M.; Martínez, S.; Serre, C.; Gómez, E.; Pérez-Rodríguez, A.; Vallés, E. Design and electrochemical preparation of inductive copper coils for magnetic particles detection. *Sens. Actuators B Chem.* **2012**, *173*, 737–744. [CrossRef]
4. Isa, N.N.C.; Mohd, Y.; Zaki, M.H.M.; Mohamad, S.A.S. Characterization of Copper Coating Electrodeposited on Stainless Steel Substrate. *Int. J. Electrochem. Sci.* **2017**, *12*, 6010–6021. [CrossRef]
5. Mladenović, I.O.; Lamovec, J.S.; Vasiljević-Radović, D.G.; Vasilić, R.; Radojević, V.J.; Nikolić, N.D. Implementation of the Chicot-Lesage Composite Hardness Model in a Determination of Absolute Hardness of Copper Coatings Obtained by the Electrodeposition Processes. *Metals* **2021**, *11*, 1807. [CrossRef]
6. Popov, K.I.; Djokić, S.S.; Nikolić, N.D.; Jović, V.D. *Morphology of Electrochemically and Chemically Deposited Metals*; Springer International Publishing: New York, NY, USA, 2016. [CrossRef]
7. Chen, Q.; Wang, Z.; Cai, J.; Lui, L. The influence of ultrasonic agitation on copper electroplating of blind-vias for SOI three-dimensional integration. *Microelectron. Eng.* **2010**, *87*, 527–531. [CrossRef]
8. Yokoi, M. Suppression Effect and Additive Chemistry. In *Copper Electrodeposition for Nanofabrication of Electronics Devices*; Kondo, K., Alkolkar, R.N., Barkey, D.P., Yokoi, M., Eds.; Springer: New York, NY, USA, 2014; Volume 171, pp. 27–40. [CrossRef]
9. Mladenović, I.; Bošković, M.; Lamovec, J.; Vuksanović, M.; Nikolić, N.D.; Radojević, V.; Vasiljević-Radović, D. Structural, Electrical and Mechanical Behavior of Thin Copper Coatings Obtained by Various Electrodeposition Processes. In Proceedings of the International Conference on Microelectronics (MIEL), Niš, Serbia, 12–14 September 2021.
10. Hasegawa, M.; Nonaka, Y.; Negishi, Y.; Okinaka, Y.; Osaka, T. Enhancement of the Ductility of Electrodeposited Copper Films by Room-Temperature Recrystallization. *J. Electrochem. Soc.* **2006**, *153*, C117. [CrossRef]
11. Bonou, L.; Eyraud, M.; Denoyel, R.; Massiani, Y. Influence of additives on Cu electrodeposition mechanisms in acid solution: Direct current study supported by non-electrochemical measurements. *Electrochim. Acta* **2002**, *47*, 4139–4148. [CrossRef]
12. Costa, J.M.; Neto, A.F.A. Ultrasound-assisted electrodeposition and synthesis of alloys and composite materials: A review. *Ultrason. Sonochem.* **2020**, *68*, 105193. [CrossRef]
13. Walker, C.T.; Walker, R. Effect of ultrasonic agitation on some properties of electrodeposits. *Electrodepos. Surf. Treat.* **1973**, *1*, 457–469. [CrossRef]
14. Hakamada, M.; Nakamoto, Y.; Matsumoto, H.; Iwasaki, H.; Chen, J.; Kusuda, H.; Mabuchi, M. Relationship between hardness and grain size in electrodeposited copper films. *Mater. Sci. Eng. A* **2007**, *457*, 120–126. [CrossRef]
15. Augustin, A.; Huilgol, P.; Udupa, K.R.; Bhat, U. Effect of current density during electrodeposition on microstructure and hardness of textured Cu coating in the application of antimicrobial Al touch surface. *J. Mech. Behav. Biomed. Mater.* **2016**, *63*, 352–360. [CrossRef]
16. Lamovec, J.; Jovic, V.; Randjelovic, D.; Aleksic, R.; Radojevic, V. Analysis of the composite and film hardness of electrodeposited nickel coatings on different substrates. *Thin Solid Films* **2008**, *516*, 8646–8654. [CrossRef]
17. Chicot, D.; Lesage, J. Absolute hardness of films and coatings. *Thin Solid Films* **1995**, *254*, 123–130. [CrossRef]
18. Lesage, J.; Pertuz, A.; Puchi-Cabrera, E.S.; Chicot, D. A model to determine the surface hardness of thin films from standard micro-indentation tests. *Thin Solid Films* **2006**, *497*, 232–238. [CrossRef]
19. Lesage, J.; Pertuz, A.; Chicot, D. A New Method to Determine the Hardness of Thin Films. *Matéria* **2004**, *9*, 13–22.
20. Lesage, J.; Chicot, D. A model for hardness determination of thin coatings from standard microindentation test. *Surf. Coat. Technol.* **2005**, *200*, 886–889. [CrossRef]
21. Tuck, J.R.; Korunsky, A.M.; Bull, S.J.; Davidson, R.I. On the application of the work-of-indentation approach to depth-sensing indentation experiments in coated systems. *Surf. Coat. Technol.* **2001**, *137*, 217–224. [CrossRef]
22. Korsunsky, A.M.; McGurk, M.R.; Bull, S.J.; Page, T.F. On the hardness of coated systems. *Surf. Coat. Technol.* **1998**, *99*, 171–183. [CrossRef]
23. Hou, Q.; Gao, J.; Li, S. Adhesion and its influence on micro-hardness of DLC and SiC films. *Eur. Phys. J. B* **1999**, *8*, 493–496. [CrossRef]

24. He, J.L.; Li, W.Z.; Li, H.D. Hardness measurement of thin films: Separation from composite hardness. *Appl. Phys. Lett.* **1996**, *69*, 1402. [CrossRef]
25. Chen, M.; Gao, J. The adhesion of copper films coated on silicon and glass substrates. *Mod. Phys. Lett. B* **2000**, *14*, 103–108. [CrossRef]
26. Magagnin, L.; Maboudian, R.; Carraro, C. Adhesion evaluation of immersion plating copper films on silicon by microindentation measurements. *Thin Solid Films* **2003**, *434*, 100–105. [CrossRef]
27. Bull, S.J.; Rickerby, D.S. New developments in the modeling of the hardness and scratch adhesion of thin films. *Surf. Coat. Technol.* **1990**, *42*, 149–164. [CrossRef]
28. Burnett, P.J.; Rickerby, D.S. The mechanical properties of wear-resistant coatings. II: Experimental studies and interpretation of hardness. *Thin Solid Films* **1987**, *148*, 51–65. [CrossRef]
29. Beegan, D.; Chowdhury, S.; Laugier, M.T. Modification of composite hardness models to incorporate indentation size effects in thin films. *Thin Solid Films* **2008**, *516*, 3813–3817. [CrossRef]
30. Magagnin, L.; Cojocar, P.; Raygani, A.; Brivio, D.; Secundo, F.; Turolla, A.; Ottolina, G. Galvanic Displacement of Nanostructured Gold for Flavoenzyme Adsorption in Biotechnology. *ECS Trans.* **2011**, *33*, 59. [CrossRef]
31. Algellai, A.A.; Tomić, N.; Vuksanović, M.M.; Dojčinović, M.; Volkov-Husović, T.; Turolla, A.; Radojević, V.; Jančić-Heinemann, R. Adhesion testing of composites based on Bis-GMA/TEGDMA monomers reinforced with alumina based fillers on brass substrate. *Compos. Part B* **2018**, *140*, 164–173. [CrossRef]
32. Tomić, N.; Saleh, M.N.; Vuksanović, M.M.; Egelja, A.; Obradović, V.; Marinković, A.; Jančić-Heinemann, R. Tailored Adhesion Properties of Acrylate Adhesives on Al Alloys by the Addition of Mn-Al-LDH. *Polymers* **2021**, *13*, 1525. [CrossRef]
33. Cemin, F.; Lundin, D. Low electrical resistivity in thin and ultrathin copper layers grown by high power impulse magnetron sputtering. *J. Vac. Sci. Technol. A* **2016**, *34*, 051506. [CrossRef]
34. Artunc, N.; Ozturk, Z.Z. Influence of grain-boundary and surface scattering on the electrical resistivity of single-layered thin copper films. *J. Phys. Condens. Matter* **1993**, *5*, 559. [CrossRef]
35. Sharma, A.; Khandelwal, S.K.; Bansal, D.; Rangra, K.; Kumar, D. Experimental study of sheet resistivity and thickness measurement for copper electroplating. In Proceedings of the International Conference NSTI-Nanotech, Santa Clara, CA, USA, 12–16 May 2013; CRC Press: Washington, DC, USA, 2013.
36. Zhang, H.P.; Jiang, Z.H.; Lian, J.S.; Hou, X.F. Surface characterization and electrical resistivity of electroless plating nanocrystalline copper films on glass. *Trans. Nonferr. Met. Soc. China* **2007**, *17*, s736–s740.
37. Standard Practice for Microetching Metals and Alloys, ASTM International, 100 Barr Harbor Drive, PO Box C700, West Conshohocken, PA 19428-2959, United States, E 407-99. Available online: https://edisciplinas.usp.br/pluginfile.php/4313805/mod_resource/content/1/NORMA_ASTM_ATAQUE_E407-99.28400.pdf (accessed on 18 December 2021).
38. Horcas, I.; Fernández, R. WSXM: A software for scanning probe microscopy and a tool for nanotechnology. *Rev. Sci. Instrum.* **2007**, *78*, 013705. [CrossRef]
39. Oliveira, F.S.; Cipriano, R.B.; da Silva, F.T.; Romão, E.C.; dos Santos, C.A.M. Simple analytical method for determining electrical resistivity and sheet resistance using the van der Pauw procedure. *Sci. Rep.* **2020**, *10*, 16379. [CrossRef]
40. Van der Pauw, L.J. A Method of Measuring the Resistivity and Hall Coefficient on Lamellae of Arbitrary Shape. *Philips Tech. Rev.* **1958**, *20*, 220–224.
41. ISO 6507-1-2005. *Metallic Materials—Vickers Hardness Test—Part 1: Test Method*; International Organization for Standardization: Geneva, Switzerland, 2005.
42. Martins, L.; Martins, J.; Romeira, A.; Costa, M.E.V.; Costa, J.S.; Bazzouai, M. Morphology of copper coatings electroplated in an ultrasonic field. *Mater. Sci. Forum* **2004**, *455–456*, 844–848. [CrossRef]
43. Naftaly, M.; Das, S.; Gallop, J.; Pan, K.; Alkhalil, F.; Kariyapperuma, D.; Constant, S.; Ramsdale, C.; Hao, L. Sheet Resistance Measurements of Conductive Thin Films: A Comparison of Techniques. *Electronics* **2021**, *10*, 960. [CrossRef]
44. Pavlović, M.G.; Pavlović, L.R.; Doroslovački, I.D.; Nikolić, N.D. The effect of benzoic acid on the corrosion and stabilization of electrodeposited copper powder. *Hydrometallurgy* **2004**, *73*, 155–162. [CrossRef]
45. Mladenović, I.O.; Lamovec, J.S.; Vasiljević Radović, D.G.; Vasilčić, R.; Radojević, V.J.; Nikolić, N.D. Morphology, Structure and Mechanical Properties of Copper Coatings Electrodeposited by Pulsating Current (PC) Regime on Si(111). *Metals* **2020**, *10*, 488. [CrossRef]
46. Mladenović, I.O.; Nikolić, N.D.; Lamovec, J.S.; Vasiljević Radović, D.G.; Radojević, V.J. Application of the Composite Hardness Models in the Analysis of Mechanical Characteristics of Electrolytically Deposited Copper Coatings: The Effect of the Type of Substrate. *Metals* **2021**, *11*, 111. [CrossRef]
47. Nikolić, N.D.; Rakočević, Z.; Popov, K.I. Structural Characteristics of Bright Copper Surfaces. *J. Electroanal. Chem.* **2001**, *514*, 56–66. [CrossRef]
48. Panda, B.; Das, S.C.; Panda, R.K. Effect of added cobalt ion on electro-deposition of copper from sulfate bath using graphite and Pb–Sb anodes. *Hydrometallurgy* **2009**, *95*, 87–91. [CrossRef]
49. Liang, X.; Ren, X.; He, R.; Ma, T.; Liu, A. Theoretical and experimental study of the influence of PEG and PEI on copper electrodeposition. *New J. Chem.* **2021**, *45*, 19655–19659. [CrossRef]
50. Plieth, W. Additives in the electrocrystallization process. *Electrochim. Acta* **1992**, *37*, 2115–2121. [CrossRef]

51. Muresan, L.M.; Varvara, S.C. Leveling and Brightening Mechanisms in Metal Electrodeposition. In *Metal Electrodeposition*; Nunez, M., Ed.; Nova Science Publishers, Inc.: New York, NY, USA, 2005.
52. Mladenović, I.O.; Lamovec, J.S.; Vasiljević-Radović, D.G.; Radojević, V.J.; Nikolić, N.D. Determination of the absolute hardness of electrolytically produced copper coatings by application of the Chicot-Lesage composite hardness model. *J. Serb. Chem. Soc.* **2022**, *86*, 105. [[CrossRef](#)]
53. Mladenović, I.O.; Lamovec, J.S.; Vasiljević-Radović, D.G.; Radojević, V.J.; Nikolić, N.D. Mechanical features of copper coatings electrodeposited by the pulsating current (PC) regime on Si(111) substrate. *Int. J. Electrochem. Sci.* **2020**, *15*, 12173–12191. [[CrossRef](#)]
54. Ma, Z.; Zhou, Y.; Long, S.; Lu, C. On the intrinsic hardness of a metallic film/substrate system: Indentation size and substrate effects. *Int. J. Plast.* **2012**, *34*, 1–11. [[CrossRef](#)]
55. Chudoba, T.; Richter, F. Investigation of creep behaviour under load during indentation experiments and its influence on hardness and modulus results. *Surf. Coat. Technol.* **2001**, *148*, 191–198. [[CrossRef](#)]
56. Lamovec, J.; Jovic, V.; Aleksic, R.; Radojevic, V. Micromechanical and structural properties of nickel coatings electrodeposited on two different substrates. *J. Serb. Chem. Soc.* **2009**, *74*, 817–831. [[CrossRef](#)]
57. Petřík, J.; Blaško, P.; Vasilňáková, A.; Demeter, P.; Futáš, P. Indentation size effect of heat treated aluminum alloy. *Acta Met. Slovaca* **2019**, *25*, 166–173. [[CrossRef](#)]
58. Li, H.; Bradt, R.C. Knoop microhardness anisotropy of single-crystal LaB₆. *Mater. Sci. Eng. A* **1991**, *142*, 51–61. [[CrossRef](#)]
59. Bull, S.J. Microstructure and indentation response of TiN coatings: The effect of measurement method. *Thin Solid Films* **2019**, *688*, 137452. [[CrossRef](#)]
60. Pan, H.; He, Y.; Zhang, X. Interactions between Dislocations and Boundaries during Deformation. *Materials* **2021**, *14*, 1012. [[CrossRef](#)] [[PubMed](#)]
61. Zhang, W.; Brongersma, S.H.; Clarysse, T.; Terzieva, V.; Rosseel, E.; Vandervorst, W.; Maex, K. Surface and grain boundary scattering studied in beveled polycrystalline thin copper films. *J. Vac. Sci. Technol. B* **2004**, *22*, 1830. [[CrossRef](#)]
62. Lee, H.; Chen, C.M. Impurity Effects in Electroplated-Copper Solder Joints. *Metals* **2018**, *8*, 388. [[CrossRef](#)]
63. Chang, S.C.; Shieh, J.M.; Dai, B.T.; Feng, M.S.; Li, Y.H. The Effect of Plating Current Densities on Self-Annealing Behaviors of Electroplated Copper Films. *J. Electrochem. Soc.* **2002**, *149*, G535–G538. [[CrossRef](#)]